Analysis of protein glycosylation after rapid digestion using protease-containing membranes in spin columns

Weikai Cao[1] and Merlin L. Bruening[1,2*]

[1]Department of Chemical and Biomolecular Engineering, University of Notre Dame, Notre Dame, Indiana 46556, United States

[2]Department of Chemistry, University of Notre Dame, Notre Dame, Indiana 46556, United States

*Corresponding author: mbruenin@nd.edu

ABSTRACT: Glycosylation is an important protein post-translational modification that plays a pivotal role in the bio-activity of therapeutic proteins and in the infectivity of viral proteins. Liquid chromatography with tandem mass spectrometry readily identifies protein glycans with site specificity. However, the overnight incubation used in conventional in-solution proteolysis leads to high turnaround times for glycosylation analysis, particularly when sequential in-solution digestions are needed for site-specific glycan identification. Using bovine fetuin as a model glycoprotein, this work first shows that in-membrane digestion in ~3-min yields similar glycan identification and quantitation when compared to overnight in-solution digestion. Protease-containing membranes in a spin column enable digestion of therapeutic proteins (Trastuzumab and erythropoietin) and a viral protein (SARS-CoV-2 Receptor Binding Domain) in ~30 sec. Glycan identification is similar after in-solution and in-membrane digestion, and limited in-membrane digestion enhances the identification of high-mannose glycans in Trastuzumab. Finally, stacked membranes containing trypsin and chymotrypsin allow fast sequential proteolytic digestion to site-specifically identify the glycans of SARS-CoV-2 Receptor Binding Domain. One can easily assemble the protease-containing membranes in commercial spin columns, and spinning multiple columns simultaneously will facilitate parallel analyses.

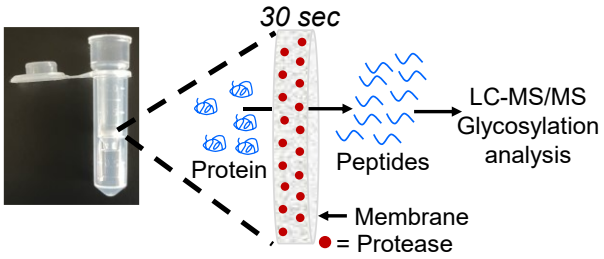

INTRODUCTION

Glycosylation is a complex protein post-translational modification (PTM) because of the many possible glycan compositions as well as glycan modifications such as methylation, acetylation, and phosphorylation.[1] Aberrant protein glycosylation plays an important role in cancer. [2,3] For example, Saldova and coworkers found an increase of core-fucosylated biantennary glycans and α2-3-linked sialic acids in the serum N-glycomes of men with prostate cancer compared to those with benign prostatic hyperplasia.[4] Catarina and coworkers demonstrated an association between aberrant O-glycosylation in serum proteins and precursor lesions of gastric carcinoma.[5]

Additionally, control over glycosylation is important for maintaining the bioactivity and stability of protein drugs. Therapeutic antibodies carrying high-mannose glycans on their crystallizable fragment region are more likely to be cleared from human serum.[6] This clearance may stem from binding to mannose receptors on sinusoidal endothelium cells in the liver.[7] Several computational studies proposed that the glycosylation of antibodies affects glycan-glycan and glycan-protein interactions to alter the antibody structure and impact its functionality.[8,9] For erythropoietin, which is used to treat anemia, the sialic acid content, the number of antennary structures, and the extent of O-acetylation (Ac) of sialic acids affect its pharmacokinetics.[10] The distribution half-time of desialated erythropoietin in rat serum decreased from ~50 min to ~5 min compared to unmodified erythropoietin.[11] Acetylation of sialic acid partially protects these species from Newcastle disease virus sialidase.[12] Finally, glycosylation also plays a pivotal role in shielding virus epitopes from cell/antibody recognition.[13,14]

Proteolysis of glycoproteins followed by liquid chromatography with tandem mass spectrometry (LC-MS/MS) is one of the important methods for identifying glycosylation sites and glycan composition.[15] Proteases employed in this method include trypsin, chymotrypsin, Glu-C, and Operator, a protease the specifically cleaves proteins after glycosylated serine and threonine residues.[16] Although LC-MS/MS analysis of proteolytic glycopeptides avoids time-consuming derivatization of glycans to improve their ionization,[17] proteolytic digestion prior to LC-MS/MS may take more than 16 hours. This greatly increases the turnaround time for glycopeptide analysis *via* LC-MS/MS. A series of enzyme-containing materials were developed to decrease digestion times. These include monoliths,[18,19] electro-spun nanofibers,[20] magnetic nanoparticles,[21,22] capillaries,[23] and membranes.[24,25] Modification of membranes can occur particularly simply by flowing polyelectrolyte- and enzyme-containing solutions through the membrane.[24]

Furthermore, diverse platforms such as spin columns,[26] microchips,[27] and pipette tips[28] can facilitate proteolysis.

Ekström and coworkers designed an automatic sampling system that couples with microchips to enhance sample digestion, but the fabrication of these chips involves several steps accomplished in a clean room.[27] Commercial spin columns contain trypsin immobilized on beads, but digestion times are typically 15-30 min.[29,30] Flow through membrane pores enables particularly rapid digestion.

This paper describes the use of protease-containing membrane spin columns to digest proteins in minutes prior to site-specific identification of glycans. These analyses would typically employ isolated or enriched proteins to limit complexity. Rapid characterization of glycosylation could facilitate quality control when manufacturing therapeutic proteins.[31] We previously used enzyme-containing spin membranes for digesting proteins before analysis of amino acid sequence variations and PTMs.[25] The spin membranes were assembled by Takara Bio USA. This research focuses on rapid digestion for glycan analysis. Moreover, to simplify the process, we now manually introduce the membranes in empty spin columns.[32] During centrifugation of spin columns, proteins flow through the membrane within 30 seconds to yield proteolytic peptides for subsequent LC-MS/MS. This short digestion enables glycan identification similar to that after in-solution digestion for 16 h. Moreover, deliberately limiting tryptic in-membrane digestion enhances the detection of some low-abundance glycans in Trastuzumab. Finally, we employ tandem trypsin- and chymotrypsin-containing membranes in a spin column to profile the site-specific glycosylation of SARS-CoV-2 Receptor Binding Domain (one O-glycosite and two N-glycosites).

EXPERIMENTAL SECTION

Chemicals and Materials. Trypsin (TPCK-treated, lyophilized powder, ≥10 000 BAEE units per mg of protein), chymotrypsin (Type II, TLCK treated to inactivate residual trypsin activity), PSS (poly(sodium 4-styrenesulfonate), average molecular weight ~70,000), fetuin from fetal bovine serum (catalog number F3004), urea, dl-1,4-dithiothreitol (DTT), iodoacetamide (IAA), and 2-bromoethanolamine were purchased from Sigma-Aldrich. Sequencing grade modified trypsin and chymotrypsin for in-solution digestion were obtained from Promega. Nylon membranes (LoProdyne LP, nominal pore size 1.2 μm, 110 μm thickness) were acquired from Pall Corporation. Trastuzumab (Herceptin, Genentech) and was diluted from its commercial formulation. Recombinant human erythropoietin (rhEPO) was acquired from GenScript, and recombinant SARS-CoV-2, S1 Subunit Protein (RBD) was purchased from RayBiotech. Empty spin columns were obtained from Bio-Rad. Solutions were prepared in deionized water (DI water, Milli-Q, 18.2 MΩ cm at 25 °C). Amicon ultra 0.5 mL centrifugal filters (MWCO of 10 kDa) were employed to desalt reduced and alkylated (or aminoethylated) proteins prior to in-membrane or in-solution digestion.

Modification of Membranes with Proteases. Membranes were cleaned with UV/ozone (Jelight model 18) for 10 min and then rinsed with 10 mL of DI water. Membrane modification occurred at room temperature. Ten mL of 3.7 mg/mL PSS in 0.5 M NaCl (pH = 2.3) was subsequently circulated through the membrane for 20 min using a peristaltic pump, followed by rinsing with passage of 30 mL of DI water. For trypsin-containing membranes, after adsorption of PSS and rinsing, 1 mL of 1 mg/mL trypsin (TPCK-treated) in 2.7 mM HCl was circulated through the membrane for 30 min. Subsequently, the membrane was rinsed with 30 mL of 1 mM HCl, dried with N_2, and stored in a fridge. For chymotrypsin-containing membranes, 1 mL of 1 mg/mL chymotrypsin in 2.7 mM HCl and 2 mM $CaCl_2$ was circulated through the PSS-modified membrane for 30 min. Then, the membrane was rinsed with 30 mL of 1 mM HCl, dried with N_2, and stored in a fridge. Flow rates during membrane modification were 1 mL/min through a membrane with an exposed area of 3.1 cm^2. We stored the membrane at 4 °C, but digestion took place at room temperature.

Protein Reduction, Alkylation and Digestion. The target protein (Fetuin, Trastuzumab or SARS-CoV-2 RBD, ~10 μL of 2 mg/mL protein, total mass of 20 μg) was added to 50 μL of solution containing 8 M urea and 50 mM ammonium bicarbonate (pH = ~8.5). Three μL of 16 mg/mL DTT (dissolved in DI H_2O) was added and the solution was incubated at 37 °C for 1 hour. After that, 11 μL of 18 mg/mL iodoacetamide was added, and the solution was incubated for 30 minutes in the dark at room temperature. 400 μL of 50 mM ammonium bicarbonate was added to the solution, which was subsequently transferred to a 10K filter for desalting in two centrifugation steps, with ~30 μL of retentate after each centrifugation. The desalted protein was diluted to 0.1 mg/mL in 50 mM ammonium bicarbonate (total volume of 200 μL) prior to in-membrane digestion or in-solution digestion. For tryptic or chymotryptic in-solution digestion, sequencing-grade trypsin or chymotrypsin was added to the reduced and alkylated protein at a mass ratio of 1:50, and the mixture was incubated at 37 °C for ~16 hours. For tryptic in-membrane digestion of fetuin, 100 μL of 0.1 mg/mL reduced and alkylated fetuin was passed through a 0.021 cm^2 trypsin-containing membrane at 2.0 mL/hour with a syringe pump.[24] For tryptic or chymotryptic in-membrane digestion of Trastuzumab, rhEPO or SARS-CoV-2 RBD, 50 μL of 0.1 mg/mL reduced and alkylated protein was passed through trypsin- or chymotrypsin-membrane spin columns at 500 *g* for 30 seconds. Digested protein was dried and dissolved in 25 μL of an aqueous solution containing 4 vol% acetonitrile and 0.1 vol% formic acid prior to LC-MS/MS. For the rhEPO reduction and aminoethylation, we followed an adapted literature procedure.[33] First, the rhEPO (25 μg in 125 μL of 20 mM phosphate buffer with 150 mM NaCl) was added to 300 μL of 10 mM ammonium bicarbonate. This solution was added to a 10 K filter to concentrate the protein to a volume of ~20 μL. This step also removes salt from the buffer. Subsequently, the concentrated sample was added to 50 μL of a solution containing 8 M Guanidine and 0.2 M Tris (pH = ~8.5). Three μL of 16 mg/mL DTT (dissolved in DI H_2O) was added, and the solution was incubated at 37 °C for 1 hour. Then, 11 μL of 36 mg/mL 2-bromoethanolamine (dissolved in DI H_2O) was added to the solution, and the mixture was incubated for an additional hour in the dark at 60 °C. As above, 400 μL of 50 mM ammonium bicarbonate was added to achieve a final volume of ~500 μL, and the solution was desalted using a 10 K filter (two centrifugation steps, with ~30 μL of retentate after each centrifugation) and diluted to a final

concentration of 0.1 mg rhEPO per mL in 50 mM ammonium bicarbonate for digestion.

Glycopeptide Analysis Using Nano LC–MS/MS. Digested proteins (1.0 μL of 0.2 mg/mL protein, assuming no sample loss) were separated on a 100 mm × 75 μm C18-BEH column (Waters, Billerica, MA) using a 48-min gradient from 4 to 33% B. Solvent A was 0.1% formic acid in DI water, and solvent B was CH_3CN. The separation employed a nano-Acquity system (Waters) with a flow rate of 900 nL/min. Glycopeptides were analyzed using a Q-Exactive HF (Thermo Scientific) mass spectrometer with an electrospray ionization voltage of 3 kV. The MS method used the following parameters: MS scan range (m/z) = 400–2000; resolution = 120,000; AGC target = 2.0e5; maximum injection time = 100 ms; included charge state = 2–5; dynamic exclusion duration = 15 s. The MS/MS method consisted of a top 17 data-dependent acquisition (DDA) mode in which all MS/MS dissociations were performed with stepped higher energy collisional dissociation (step-HCD): resolution = 15,000; AGC target = 5.0e5; maximum injection time = 250 ms; stepped collision energy = 20%, 30%, 40%. For the tandem-membrane digests and rhEPO digests, the stepped collision energy was adjusted to 15%, 25%, 35%.

Data Analysis. The raw data obtained from the mass spectrometer were analyzed using GlycoDecipher.[34] The parameters were set as: fixed modification (Carbamidomethyl, C, +57.022 Da), variable modifications (Acetyl, proteinN-term, +42.011 Da), max missed cleavages (3), precursor tolerance (5 ppm), fragment tolerance (20 ppm), enzyme (tryptic digestion: KR, chymotryptic digestion: FY, tandem chymotryptic and tryptic digestion: FYR- there is no K near the glycosylation sites). For rhEPO, the parameters were modified to include: fixed modification (Ethanolamine, C, +43.042 Da) and tryptic digestion: KRC. The quantitation of glycopeptides was obtained from the label-free quantitation function of Glyco-Decipher.[34] The protein database (bovine fetuin, SARS-CoV-2 RBD or rhEPO) was downloaded from UniprotKB while the protein database of Trastuzumab was downloaded from KEGG. The glycopeptide fragmentation spectrum of SARS-CoV-2 RBD was labelled using pGlyco3.0.[35] The terminology for describing glycans includes Hex=hexose; HexNAc=N-Acetylhexosamine; NeuAc=N-Acetyl-Neuraminic Acid; NeuGc= N-Glycolylneuraminic acid; NeuAc_Ac= mono-acetylated N-Acetyl-Neuraminic Acid; NeuAc_2Ac= dual-acetylated N-Acetyl-Neuraminic Acid; pHex=phosphorylated hexose. The numbers in parentheses after each sugar denote how many units of the sugar exist in the glycan.

We manually examined the glycopeptide identifications and interpreted the glycopeptide fragmentation spectra of certain replicate analyses of Trastuzumab, rhEPO and SARS-CoV-2 RBD.[36] The most common cause of incorrect identifications was erroneous assignment of the monoisotopic mass. The mass of two fucoses is very close to the mass of one sialic acid (mass difference of 1 Da). Therefore, the determination of the monoisotopic mass is vital for differentiating glycans containing two fucose moieties from those containing sialic acids. The glycopeptide retention time for glycans containing one sialic acid is larger than that for glycans with two fucose-containing species (Table S-1), which agrees with previous reports.[37,38] Thus, retention times can serve as a criterion for confirming the interpretation of MS and MS/MS spectra. Furthermore, the mass of 1*HexNAc-1*Hex (41.03 Da) is also very close to sialic acid acetylation (42.01 Da). In some cases, Glyco-Decipher misinterpreted the glycans containing acetylated sialic acids as those not containing acetylated sialic acids (e.g., Hex(6)HexNAc(5)NeuAc(2)NeuAc(1)NeuAc_Ac(1)Fuc(1) as Hex(5)HexNAc(6)NeuAc(3)Fuc(1)). The third cause for misidentification is coelution of glycopeptides with similar masses. In this case, the MS/MS spectrum can contain signals for two different peptides, which greatly complicates interpretation.

For manual verification and interpretation, we first examined the low-mass range (m/z=180-800) MS/MS spectrum to confirm the presence of different sugar types (e.g., to demonstrate the presence of ions of sialic acid-m/z 292 and 274, phosphorylated hexose-m/z 243 and 225, mono-acetylated sialic acid-m/z 316 and 334, or dual-acetylated sialic acid-m/z 358 and 376). The software does not seem to take these signals into account. Relative intensities also suggest whether there are multiple sialic acids, phosphorylated hexoses, or acetylated sialic acids. If the intensities or sugar types were inconsistent with the software-identified composition, we re-interpreted the MS/MS spectrum with a 1 or 2 Da decrease in monoisotopic mass. For a monoisotopic mass drop of 2 Da, the signal of sialic acid should be relatively high. Additionally, we also deduced the number of sialic acids by the glycopeptide retention time compared to other more intense glycan compositions with a certain number of sialic acids. Similar glycan compositions with a higher number of sialic acids usually display a longer retention time than those with a lower number of sialic acids. In some cases manual examination revealed additional glycopeptides when the retention times of glycopeptides with the same backbone were similar.[39] When the monoisotopic mass difference between two possible glycopeptides corresponded to the mass of a specific sugar moiety (e.g., 203.08 (N-acetylglucosamine), 162.05 (hexose), 291.10 (N-acetylneuraminic acid), or 365.13 (N-acetylglucosamine and hexose)), we then examined the MS2 spectrum of the unidentified glycopeptide to see if it matched the expected composition.

RESULTS AND DISCUSSION

This section explores the utility of in-membrane digestion for site-specific glycan identification using reversed-phase LC-MS/MS analysis of single proteins. The rapid digestion procedure may enable more timely quality control during protein manufacturing.[40,41] Hydrophilic interaction chromatography could also prove useful in glycopeptide analysis but is beyond the scope of this work.[42] First, we compare tryptic in-membrane and in-solution digestion for the analysis of fetuin glycosylation. Second, we use membranes for limited digestion of Trastuzumab to enhance the identification of high-mannose glycans. Third, this research uses trypsin-containing membranes to site-specifically identify erythropoietin glycosylation. Finally, we employ tandem trypsin- and chymotrypsin-containing membranes to rapidly digest SARS-CoV-2 RBD protein for site-specific identification of glycosylation.

Comparison of glycan identification after tryptic in-membrane and in-solution digestion of fetuin. To show that trypsin-containing membranes can serve as a rapid alternative to conventional in-solution digestion, we first compare site-specific identification of glycans on bovine fetuin, a glycosylated protein that researchers often use when developing techniques for glycopeptide analysis.[43] Figure 1 shows that both proteolysis methods enable identification of 20 common glycans at the Asn99 site. In-solution digestion and in-membrane digestion identify 1 or 2 additional glycans. The Asn156 site shows a similarly high overlap between glycans identified after in-solution and in-membrane digestion (Figure 1). Tables S2-S13 list the bovine fetuin glycopeptides identified. In experiments with three different membranes, 60-75% of the total identified glycans appeared in all replicate experiments. In-solution digestion gives 60% replication (Figure S-1).

Quantitation of glycans based on glycopeptide MS1 intensities is challenging due to widely varying ionization efficiencies, including differences among sialylated, multi-sialylated, and non-sialylated species.[44] Nevertheless, Figure 2 compares the integrated intensities for the most abundant glycans.

The error bars in (A) indicate a coefficient of variation of 4-16% for 3 replicate analyses of Asn99 glycopeptides by in-membrane digestion and 10-14% for 3 replicate analyses of Asn99 glycopeptides by in-solution digestion. The error bars in (B) indicate a coefficient of variation of 2-9% for 3 replicate analyses of Asn156 glycopeptides by in-solution digestion, whereas the coefficient of variation for 3 replicate analyses of Asn156 glycopeptides by in-membrane digestion is higher, ranging from 12-33%. In-membrane and in-solution digestion give similar peak areas, but nonspecific binding to the membrane might give a modest decrease in peak areas in some cases. Overall, the 3-min in-membrane digestion is essentially as good as overnight in-solution digestion in terms of the identification and the relative quantification of unique glycans.

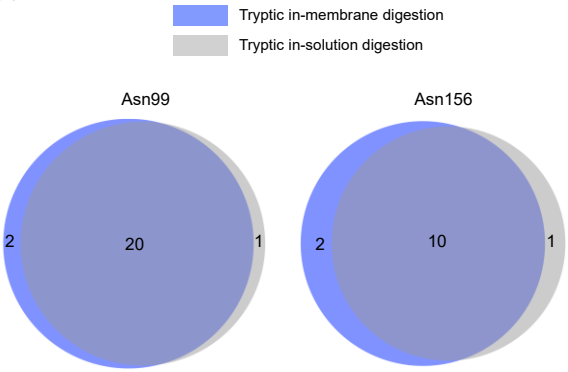

Figure 1. Comparison of the bovine fetuin glycans identified after tryptic in-membrane and in-solution digestion. The figure only shows glycans identified in all replicate experiments with three different membranes or three different in-solution digestions. Glycans were identified using Glyco-Decipher.[34]

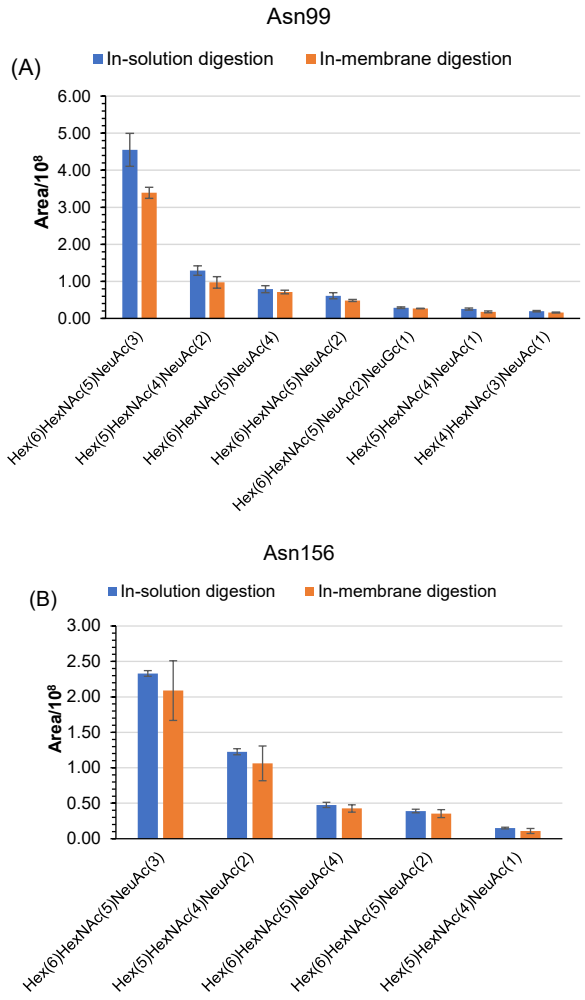

Figure 2. Comparison of the integrated areas in extracted-ion-current chromatograms of selected groups of bovine fetuin glycopeptides identified at (A) Asn99 and (B) Asn156 after tryptic in-solution (blue bars) and in-membrane (orange bars) digestion. When a single glycan appeared on two peptides, areas are sums. Only the most abundant glycans are shown. Error bars represent standard deviations from experiments with three different in-membrane or in-solution digestions.

Comparison of glycan identification after in-membrane and in-solution tryptic digestion of erythropoietin. To further compare in-membrane digestion to in-solution digestion, we employed trypsin membranes embedded in spin columns to digest recombinant human erythropoietin (rhEPO) for identification of glycosylation patterns. rhEPO possesses N-glycosylation sites at Asn51 and Asn65. However, there are no tryptic or chymotryptic cleavage sites between Asn51 and Asn65, so we followed a literature procedure and used aminoethylation of cysteine to introduce tryptic cleavage sites between these residues (Scheme 1).[33,45]

In-solution and in-membrane tryptic digestion of aminoethylated rhEPO lead to overlapping identification of 18 common N-glycans at Asn51 and 29 common N-glycans at Asn65 (Figure 3). Both types of digestion identified a few additional unique glycans at Asn51. In addition, in-membrane digestion identified more unique glycans (9) than in-solution digestion (2) at Asn65.

However, as for glycan identification at Asn110, in-solution digestion performs better (14 unique glycans) than in-membrane digestion (2 unique glycans) (Figure S-2). Overall, rapid in-membrane digestion can be comparable to overnight in-solution digestion in terms of glycan identifications, although there were some identification discrepancies between these two digestion methods in the case of rhEPO.

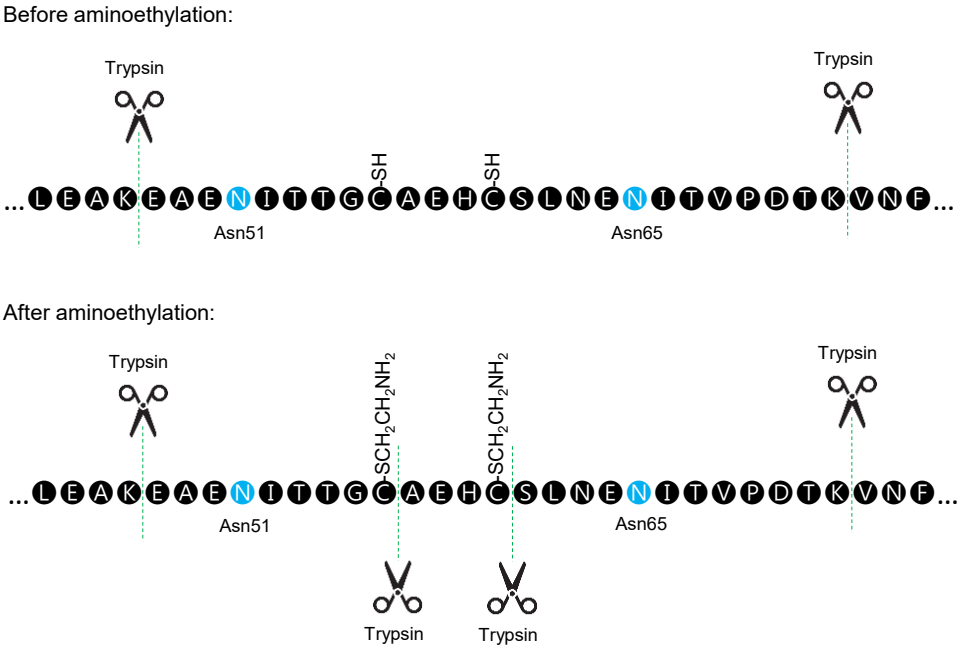

Scheme1. Introduction of additional tryptic cleavage sites in rhEPO via cysteine aminoethylation.

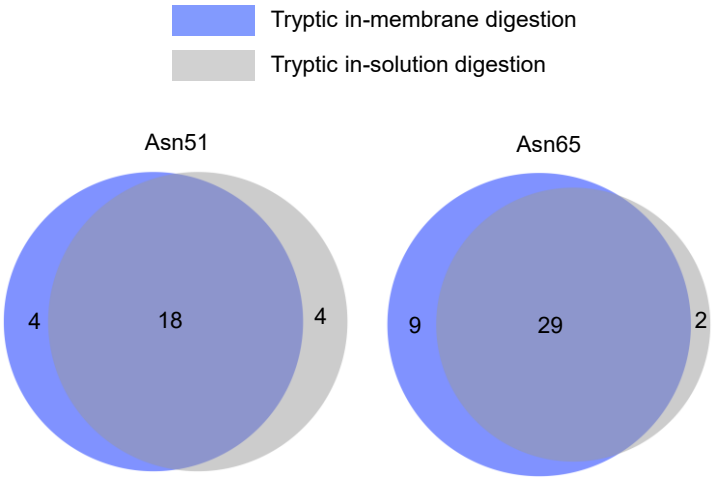

Figure 3. Comparison of the rhEPO glycans identified after tryptic in-membrane and in-solution digestion. The figure only shows glycans that appeared 4 or more times in replicate experiments with five different in-membrane digestions or in-solution digestions (Table S14-S17). Glycopeptides were identified using Glyco-Decipher[34] and additional manual identification.

Limited digestion to enhance high-mannose glycan identification in Trastuzumab. In addition to greatly decreasing digestion times, rapid flow through a trypsin-containing membrane can result in missed cleavages that enhance some analyses. Missed cleavages can lead to long and highly-charged peptides that have high ionization efficiencies and extensive fragmentation in many cases. To create long peptides, we rapidly passed solutions through membranes embedded in spin columns. Flow of 50 µL of reduced and alkylated protein through a spin membrane with an area of ~0.3 cm^2 occurs within 30 seconds of centrifugation. To further decrease the digestion rate, we sequentially flowed two fresh aliquots of intact protein through the same membrane. Passage of the first aliquot of protein through the membrane partially desorbs the trypsin (Figure S-3). Thus, the second aliquot of intact protein should undergo less digestion and contain more missed cleavages. A control experiment (Figure S-4) showed that the desorbed trypsin did not significantly digest protein in the effluent solution.

We selected Trastuzumab as an example of a common therapeutic antibody. The amino acid sequence of the crystallizable region, which carries the glycan, is very similar or identical to other humanized or partially humanized antibodies (e.g., Bevacizumab, Rituximab). Thus, the results with Trastuzumab (limited digestion to enhance high-mannose glycan identification in Trastuzumab and semiquantitative determination of glycan composition, see below) will likely apply to other therapeutic antibodies.

Trastuzumab contains glycans only at N297, and tryptic in-membrane digestion yields two dominant glycopeptide backbones: EEQYNSTYR and TKPREEQYNSTYR. As Figure 4 shows, the first aliquot passed through the membrane gives dominant signals for EEQYNSTYR peptides, whereas the second aliquot gives dominant signals for TKPREEQYNSTYR. Figures S-5, S-6, and S-7 show extracted-ion-current chromatograms for other glycopeptides, further confirming that the fraction of TKPREEQYNSTYR is larger in the second aliquot passed through the membrane. Figure 5 shows that the fraction of non-glycosylated peptides with one or more missed cleavages increases from 16% to 39% on going from the first to the second aliquot, confirming that the second aliquot undergoes less digestion. The especially large increase in glycosylated TKPREEQYNSTYR (Figure 4) in the second aliquot suggests that glycosylation may increase the number of missed cleavages during digestion of the second aliquot.

Figure 6A compares the glycans identified in the first and second aliquots of fresh Trastuzumab passed through the same spin membrane. Table S-22 lists the glycopeptides. We identified high-mannose glycans (≥6 hexoses: Hex(6)HexNAc(2), Hex(7)HexNAc(2), Hex(8)HexNAc(2) and Hex(6)HexNAc(3)) only in the second aliquot and only with the peptide backbone TKPREEQYNSTYR. (Hexoses are typically mannose in therapeutic antibodies.[46]) We did not see signals for high-mannose glycans for either the long or short peptide in the first aliquot passed through the membrane. High-mannose glycans are not abundant in therapeutic antibodies, and their high hydrophilicity[47] may decrease the ionization efficiency of glycopeptides. Due to its higher number of basic amino acid residues, glycosylated TKPREEQYNSTYR should ionize more efficiently than glycosylated EEQYNSTYR. Although both of these peptides likely carry high-mannose glycans, the mass spectrometer may only detect these high-mannose glycopeptides in the case of TKPREEQYNSTYR. Figures S-8 to S-25 show the MS and MS/MS spectra of all the identified TKPREEQYNSTYR glycopeptides. Figures S-13, S-18, S-19, and S-22 provide MS/MS spectra of the high-mannose glycopeptides and show extensive fragmentation. TKPREEQYNSTYR and EEQYNSTYR have similar hydrophobicities (GRAVY scores of -2.56 and -2.51, respectively), so the primary difference between them is likely the number of basic residues (TKPREEQYNSTYR has two additional basic residues).[48,49] Overall, these results suggest that limited tryptic digestion can enhance the MS identification of some low-abundance glycopeptides that have low ionization efficiencies. One strategy for achieving limited digestion is to pass multiple aliquots through the membrane, and a researcher may wish to consider this possibility. However, a higher centrifugation speed would pass the solution through the membrane faster, which might also result in less digestion and more missed cleavages.[26] Variation of the digestion buffer pH could also lead to less digestion and more missed cleavages.[50]

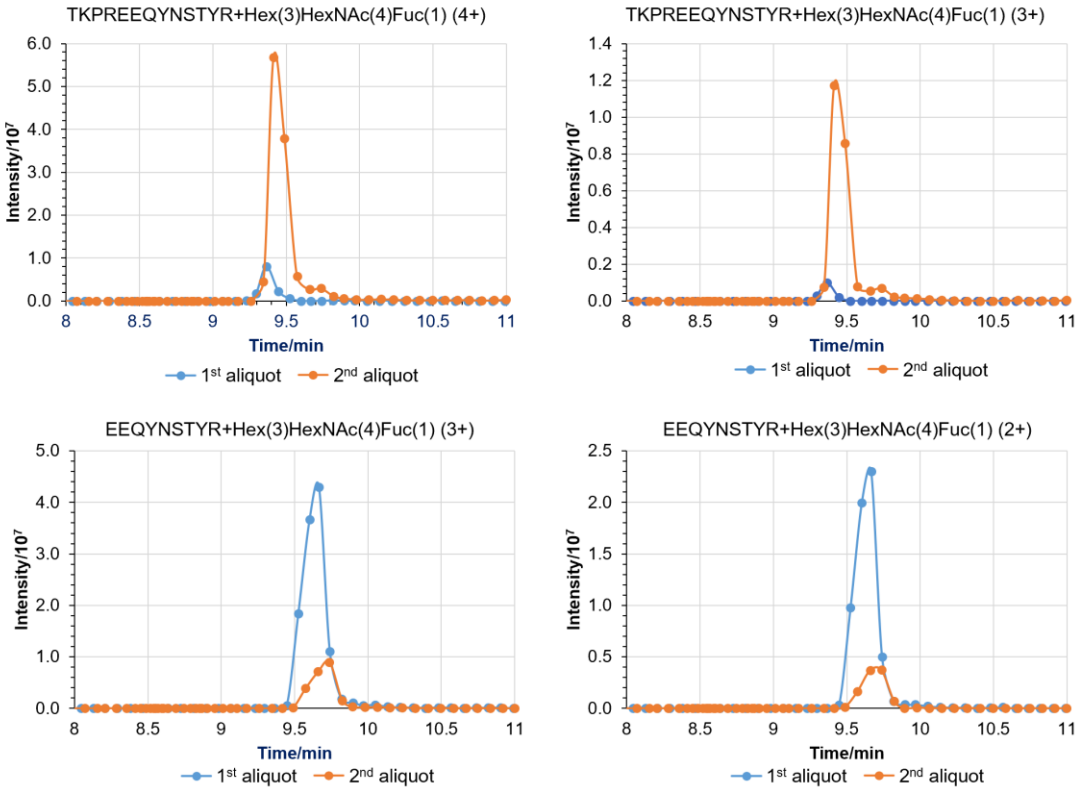

Figure 4. Extracted-ion-current chromatograms for glycopeptides with Hex(3)HexNAc(4)Fuc(1) on two different peptide backbones, TKPREEQYNSTYR and EEQYNSTYR, at different charge states. The figure compares analyses of the first (blue) and second (orange) aliquots of the Trastuzumab solution passed through the same tryptic spin membrane. The second passage gives more missed cleavages to enhance the fraction of the longer peptide. Fuc=Fucose.

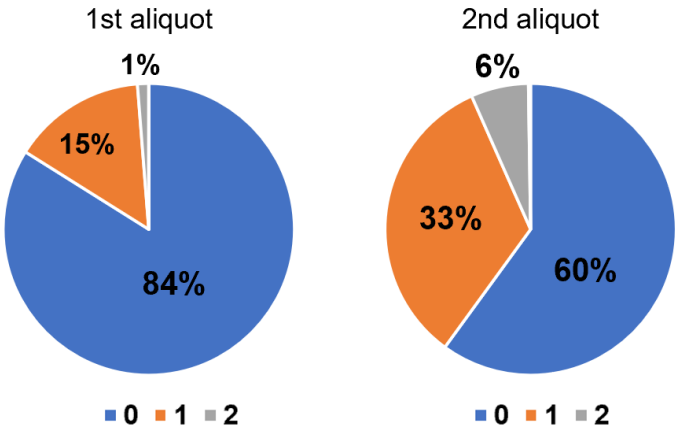

Figure 5. Percentages of identified non-glycosylated peptides with 0, 1, and 2 missed cleavages in the 1st and 2nd aliquots of fresh Trastuzumab passed through the same spin membrane. The missed-cleavage percentage is the average number from 3 replicate experiments. No identified peptides contained 3 missed cleavages. Analysis occurred using PEAKS software.

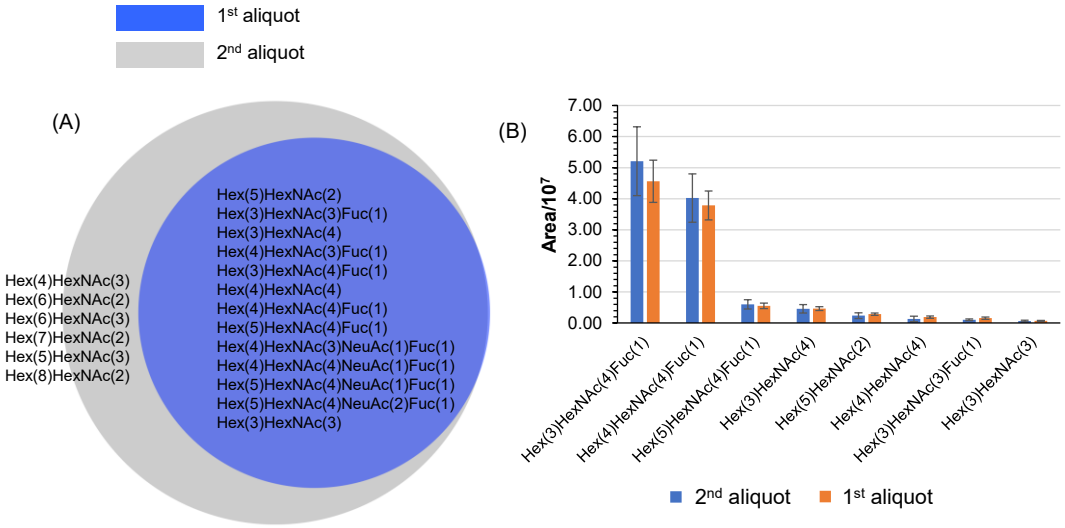

Figure 6. (A) Comparison of Trastuzumab glycans identified in the first and second aliquots of fresh Trastuzumab passed through the same membrane embedded in a spin column. The figure only shows glycans that appeared 4 or more times in replicate experiments with five different membranes (Table S-22). Glycopeptides were identified using Glyco-Decipher[34] and additional manual identification. (B) Integrated signals of the EEQYNSTYR (1st aliquot) and TKPREEQYNSTYR (2nd aliquot) glycopeptides carrying the indicated glycans (only the most abundant are shown). Error bars show standard deviations from analyses after digestions in five different membranes.

The integrated glycopeptide signal intensities in extracted ion-current chromatograms were consistent after digestions with 5 different membranes as Figure 6B shows. We examined the intensities of TKPREEQYNSTYR glycopeptides after the second passage (blue bars) because this peptide shows higher signals than EEQYNSTYR in the second aliquot. Consistent with literature studies, the Trastuzumab glycans with dominant signals are Hex(3)HexNAc(4)Fuc(1) (also denoted as G0F) and Hex(4)HexNAc(4)Fuc(1) (also known as G1F). The integrated MS1 signals of the other glycans are at least ~6-fold less than those of the dominant glycans. These trends (Figure 6B) are similar to results from prior glycan quantification on Trastuzumab,[51,52] which suggests that our trypsin-membrane spin column can achieve rapid glycan identification and relative quantitation. We also quantified the signals from EEQYNSTYR glycopeptides in the first aliquot passed through the membrane, as depicted by the orange bars in Figure 6B. These results also show the dominance of Hex(3)HexNAc(4)Fuc(1) and Hex(4)HexNAc(4)Fuc(1) glycans.

Tandem chymotrypsin- and trypsin-containing membranes enable identification of site-specific glycosylation in the SARS-CoV-2 Receptor Binding Domain (RBD). This section demonstrates the use of tandem membranes in spin columns to enable site-specific glycan analysis of SARS-CoV-2 RBD. This protein possesses two N-glycosylation sites: Asn331 and Asn343. However, there is no lysine or arginine between these two residues. Thus, trypsin digestion alone cannot distinguish between the glycans on Asn331 and Asn343 because both residues are present on the same peptide (Scheme 2). Fragmentation of the tryptic peptide will likely be insufficient to specifically identify the two glycans on this peptide.[53] The combination of tryptic and chymotryptic digestion, however, will cleave the SARS-CoV-2-RBD between all glycosylation sites. Chymotrypsin should cleave SARS-CoV-2 RBD after phenylalanine (F) residues between Asn343 and Asn331 (Scheme 2). This enzyme preferentially cleaves peptides after F, W, and Y residues. However, in addition to N-glycosylation, SARS-CoV-2 RBD possesses an O-glycosylation site at Thr323. Due to the proline following Phe329, chymotrypsin will not have a cleavage site between Thr323 and Asn331 according to the "Keil rules".[54] Consequently, fragmentation of chymotryptic peptides will be inadequate to distinguish between glycans at Thr323 and Asn331. Thus, site-specific analysis of all glycosylation sites will require the combination of trypsin and chymotrypsin.

Due to well-placed glutamic acid residues (E) surrounding the three glycosylation sites, several research groups used Glu-C to digest SARS-CoV-2 RBD and produce different peptides containing each of the glycans.[55–57] Glu-C digestions may employ overnight incubations.[58] Two studies showed that sequential in-solution digestion with trypsin and chymotrypsin leads to different peptides containing the three glycans (Scheme 2).[36,59] However, the in-solution digestion occurred for ~24 hours (trypsin digestion for 8 hours and chymotrypsin digestion for 16 hours). Therefore, this study aims to site-specifically identify the glycans on RBD using rapid digestion during passage of a protein solution through tandem chymotrypsin and trypsin membranes in a spin column (Figure 7).

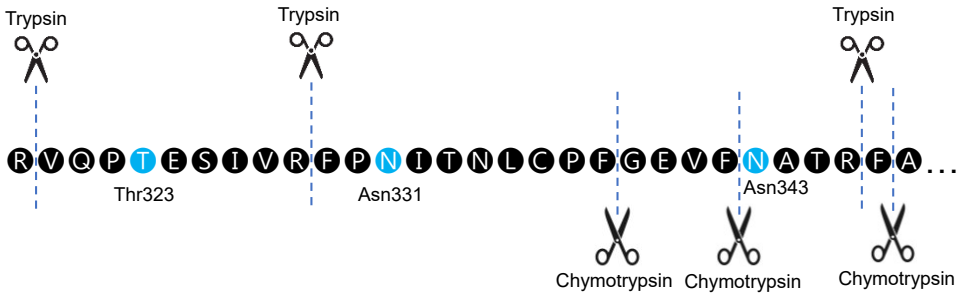

Scheme 2. Illustration of the cleavage-site differences between trypsin and chymotrypsin for SARS-CoV-2 RBD near glycosylation sites.

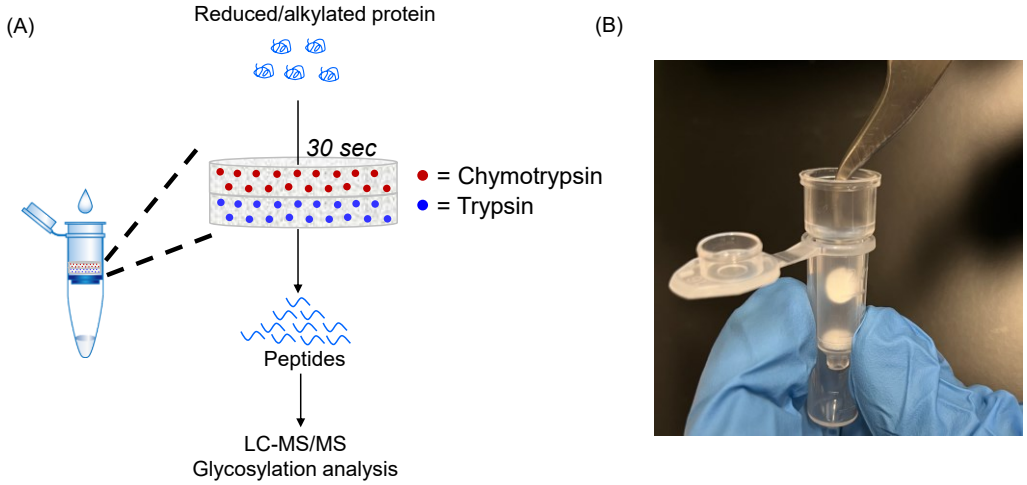

Figure 7. (A) Illustration of tandem membrane digestion. (B) Assembly of a protease-containing spin column. Two membranes were added for tandem digestion.

We first examined glycan identification after digestion with just chymotrypsin. After in-membrane chymotryptic digestion, LC-MS/MS analysis identified 29 glycans on the Asn343 site. In-solution digestion enabled reproducible identification of the same 29 glycans along with 3 additional low-abundance sugars (see Table S-23, reproducible glycan identifications include those that appeared in ≥3 of 4 replicate digestions). However, neither method for chymotrypsin digestion allowed identification of glycans on Asn331 or Thr323.

In digestion with both trypsin and chymotrypsin, we placed a chymotrypsin membrane on top of a trypsin membrane in a spin column. Digestion of SARS-CoV-2 RBD occurred during centrifugation through the membrane stack prior to LC-MS/MS analysis (Figure 7). The digestion procedure only takes ~30 seconds. Unlike digestion with just chymotrypsin, the tandem-membrane digestion enabled glycan identification at Thr323 and Asn331. Proteolysis with the tandem membranes enabled reproducible identification of 18 glycans at Asn331 and 15 glycans at Thr323, (see Tables S-24 and S-25, reproducible glycan identifications include those that appeared in ≥4 of 5 replicate digestions). Consistent with prior studies, some of the hexoses at Asn331 were phosphorylated, suggesting that Asn331 is functionalized in the Golgi apparatus.[60,61] Unfortunately, at Asn343 only 6 glycans showed reproducible identification after tandem membrane digestion (Table S-26, reproducible glycan identifications include those that appeared in ≥4 of 5 replicate digestions). This low number of identifications may occur because we did not observe glycosylated NATR. This peptide, which results from combined chymotryptic and tryptic cleavage (Scheme 2), probably does not ionize well due to its short length. Figure S-26 (A) to (C) shows examples of fragmentation patterns for peptides with glycosylation at Asn343, Asn331, and Thr323. Overall, the tandem membrane digestion effectively allows identification of glycans when a single enzyme does not afford cleavage between two glycosylation sites.

Conclusions

This study used bovine fetuin, rhEPO and SARS-CoV-2 RBD to demonstrate that in-membrane digestion results in glycan identifications that are comparable to those after in-solution digestion. However, in-membrane digestion only takes 30 seconds in spin columns. Additionally, membranes can allow limited digestion that may increase the identification of some low-

abundance glycans. A tandem membrane format provides a fast method for sequential proteolytic digestion to facilitate site-specific glycosylation analysis on SARS-CoV-2 RBD. Protease-containing membranes are relatively easy to assemble in commercial spin columns, and one can spin multiple columns simultaneously. Such spin membranes may facilitate shorter turnaround times in glycosylation analysis.

ASSOCIATED CONTENT

Supporting Information

The Supporting Information is available free of charge on the ACS Publications website and includes tables and figures of identified peptides and some retention times, MS and MS/MS spectra, and other extracted ion chromatograms. (PDF)

AUTHOR INFORMATION

Corresponding Author

* **Merlin L. Bruening** – Department of Chemical and Biomolecular Engineering, University of Notre Dame, Notre Dame, Indiana 46556, United States; orcid.org/0000-0002-4553-5143; Phone: +1 574-631-3024; Email: mbruenin@nd.edu

Author Contributions

The manuscript was written through contributions of all authors. All authors have given approval to the final version of the manuscript.

ACKNOWLEDGMENT

The authors are grateful to the National Science Foundation for funding this work (CHE-1903967). We thank Dr. Bill Boggess from the Notre Dame Mass Spectrometry and Proteomics Facility for instrument support. We thank Yuhang Chen for helping with the manual data analysis.

REFERENCES

(1) Moremen, K. W.; Tiemeyer, M.; Nairn, A. V. Vertebrate Protein Glycosylation: Diversity, Synthesis and Function. *Nat. Rev. Mol. Cell Biol.* **2012**, *13* (7), 448–462. https://doi.org/10.1038/nrm3383.

(2) Pinho, S. S.; Reis, C. A. Glycosylation in Cancer: Mechanisms and Clinical Implications. *Nat. Rev. Cancer* **2015**, *15* (9), 540–555. https://doi.org/10.1038/nrc3982.

(3) Stowell, S. R.; Ju, T.; Cummings, R. D. Protein Glycosylation in Cancer. *Annu. Rev. Pathol. Mech. Dis.* **2015**, *10* (1), 473–510. https://doi.org/10.1146/annurev-pathol-012414-040438.

(4) Saldova, R.; Fan, Y.; Fitzpatrick, J. M.; Watson, R. W. G.; Rudd, P. M. Core Fucosylation and 2-3 Sialylation in Serum N-Glycome Is Significantly Increased in Prostate Cancer Comparing to Benign Prostate Hyperplasia. *Glycobiology* **2011**, *21* (2), 195–205. https://doi.org/10.1093/glycob/cwq147.

(5) Gomes, C.; Almeida, A.; Ferreira, J. A.; Silva, L.; Santos-Sousa, H.; Pinto-de-Sousa, J.; Santos, L. L.; Amado, F.; Schwientek, T.; Levery, S. B.; Mandel, U.; Clausen, H.; David, L.; Reis, C. A.; Osório, H. Glycoproteomic Analysis of Serum from Patients with Gastric Precancerous Lesions. *J. Proteome Res.* **2013**, *12* (3), 1454–1466. https://doi.org/10.1021/pr301112x.

(6) Goetze, A. M.; Liu, Y. D.; Zhang, Z.; Shah, B.; Lee, E.; Bondarenko, P. V.; Flynn, G. C. High-Mannose Glycans on the Fc Region of Therapeutic IgG Antibodies Increase Serum Clearance in Humans. *Glycobiology* **2011**, *21* (7), 949–959. https://doi.org/10.1093/glycob/cwr027.

(7) Kogelberg, H.; Tolner, B.; Sharma, S. K.; Lowdell, M. W.; Qureshi, U.; Robson, M.; Hillyer, T.; Pedley, R. B.; Vervecken, W.; Contreras, R.; Begent, R. H. J.; Chester, K. A. Clearance Mechanism of a Mannosylated Antibody–Enzyme Fusion Protein Used in Experimental Cancer Therapy. *Glycobiology* **2007**, *17* (1), 36–45. https://doi.org/10.1093/glycob/cwl053.

(8) Buck, P. M.; Kumar, S.; Singh, S. K. Consequences of Glycan Truncation on Fc Structural Integrity. *mAbs* **2013**, *5* (6), 904–916. https://doi.org/10.4161/mabs.26453.

(9) Chen, W.; Kong, L.; Connelly, S.; Dendle, J. M.; Liu, Y.; Wilson, I. A.; Powers, E. T.; Kelly, J. W. Stabilizing the C $_{H}$ 2 Domain of an Antibody by Engineering in an Enhanced Aromatic Sequon. *ACS Chem. Biol.* **2016**, *11* (7), 1852–1861. https://doi.org/10.1021/acschembio.5b01035.

(10) Hua, S.; Oh, M. J.; Ozcan, S.; Seo, Y. S.; Grimm, R.; An, H. J. Technologies for Glycomic Characterization of Biopharmaceutical Erythropoietins. *TrAC Trends Anal. Chem.* **2015**, *68*, 18–27. https://doi.org/10.1016/j.trac.2015.02.004.

(11) Spivak, J.; Hogans, B. The in Vivo Metabolism of Recombinant Human Erythropoietin in the Rat. *Blood* **1989**, *73* (1), 90–99. https://doi.org/10.1182/blood.V73.1.90.90.

(12) Corfield, A. P.; Sander-Wewer, M.; Veh, R. W.; Wember, M.; Schauer, R. The Action of Sialidases on Substrates Containing *O* -Acetylsialic Acids. *Biol. Chem. Hoppe. Seyler* **1986**, *367* (1), 433–440. https://doi.org/10.1515/bchm3.1986.367.1.433.

(13) Walls, A. C.; Xiong, X.; Park, Y.-J.; Tortorici, M. A.; Snijder, J.; Quispe, J.; Cameroni, E.; Gopal, R.; Dai, M.; Lanzavecchia, A.; Zambon, M.; Rey, F. A.; Corti, D.; Veesler, D. Unexpected Receptor Functional Mimicry Elucidates Activation of Coronavirus Fusion. *Cell* **2019**, *176* (5), 1026-1039.e15. https://doi.org/10.1016/j.cell.2018.12.028.

(14) Walls, A. C.; Park, Y.-J.; Tortorici, M. A.; Wall, A.; McGuire, A. T.; Veesler, D. Structure, Function, and Antigenicity of the SARS-CoV-2 Spike Glycoprotein. *Cell* **2020**, *181* (2), 281-292.e6. https://doi.org/10.1016/j.cell.2020.02.058.

(15) Clerc, F.; Reiding, K. R.; Jansen, B. C.; Kammeijer, G. S. M.; Bondt, A.; Wuhrer, M. Human Plasma Protein N-Glycosylation. *Glycoconj. J.* **2016**, *33* (3), 309–343. https://doi.org/10.1007/s10719-015-9626-2.

(16) *Genovis » OpeRATOR*. https://www.genovis.com/products/glycan-profiling/operator/ (accessed 2023-03-16).

(17) Zhou, S.; Dong, X.; Veillon, L.; Huang, Y.; Mechref, Y. LC-MS/MS Analysis of Permethylated N-Glycans Facilitating Isomeric Characterization. *Anal. Bioanal. Chem.* **2017**, *409* (2), 453–466. https://doi.org/10.1007/s00216-016-9996-8.

(18) Ma, J.; Liang, Z.; Qiao, X.; Deng, Q.; Tao, D.; Zhang, L.; Zhang, Y. Organic–Inorganic Hybrid Silica Monolith Based Immobilized Trypsin Reactor with High Enzymatic Activity. *Anal. Chem.* **2008**, *80* (8), 2949–2956. https://doi.org/10.1021/ac702343a.

(19) Zhang, Z.; Sun, L.; Zhu, G.; Cox, O. F.; Huber, P. W.; Dovichi, N. J. Nearly 1000 Protein Identifications from 50 ng of *Xenopus Laevis* Zygote Homogenate Using Online Sample Preparation on a Strong Cation Exchange Monolith Based Microreactor Coupled

with Capillary Zone Electrophoresis. *Anal. Chem.* **2016**, *88* (1), 877–882. https://doi.org/10.1021/acs.analchem.5b03496.

(20) Kim, H.; Kim, H. S.; Lee, D.; Shin, D.; Shin, D.; Kim, J.; Kim, J. Microwave-Assisted Protein Digestion in a Plate Well for Facile Sampling and Rapid Digestion. *Anal. Chem.* **2017**, *89* (20), 10655–10660. https://doi.org/10.1021/acs.analchem.7b02169.

(21) Fan, Z.; Liu, T.; Zheng, F.; Qin, W.; Qian, X. An Ultrafast N-Glycoproteome Analysis Method Using Thermoresponsive Magnetic Fluid-Immobilized Enzymes. *Front. Chem.* **2021**, *9*, 676100. https://doi.org/10.3389/fchem.2021.676100.

(22) Lin, S.; Yun, D.; Qi, D.; Deng, C.; Li, Y.; Zhang, X. Novel Microwave-Assisted Digestion by Trypsin-Immobilized Magnetic Nanoparticles for Proteomic Analysis. *J. Proteome Res.* **2008**, *7* (3), 1297–1307. https://doi.org/10.1021/pr700586j.

(23) Long, Y.; Wood, T. D. Immobilized Pepsin Microreactor for Rapid Peptide Mapping with Nanoelectrospray Ionization Mass Spectrometry. *J. Am. Soc. Mass Spectrom.* **2015**, *26* (1), 194–197. https://doi.org/10.1007/s13361-014-1015-8.

(24) Xu, F.; Wang, W.-H.; Tan, Y.-J.; Bruening, M. L. Facile Trypsin Immobilization in Polymeric Membranes for Rapid, Efficient Protein Digestion. *Anal. Chem.* **2010**, *82* (24), 10045–10051. https://doi.org/10.1021/ac101857j.

(25) Pang, Y.; Wang, W.-H.; Reid, G. E.; Hunt, D. F.; Bruening, M. L. Pepsin-Containing Membranes for Controlled Monoclonal Antibody Digestion Prior to Mass Spectrometry Analysis. *Anal. Chem.* **2015**, *87* (21), 10942–10949. https://doi.org/10.1021/acs.analchem.5b02739.

(26) Liu, W.; Pang, Y.; Tan, H.-Y.; Patel, N.; Jokhadze, G.; Guthals, A.; Bruening, M. L. Enzyme-Containing Spin Membranes for Rapid Digestion and Characterization of Single Proteins. *Analyst* **2018**, *143* (16), 3907–3917. https://doi.org/10.1039/C8AN00969D.

(27) Ekström, S.; Önnerfjord, P.; Nilsson, J.; Bengtsson, M.; Laurell, T.; Marko-Varga, G. Integrated Microanalytical Technology Enabling Rapid and Automated Protein Identification. *Anal. Chem.* **2000**, *72* (2), 286–293. https://doi.org/10.1021/ac990731l.

(28) Ning, W.; Bruening, M. L. Rapid Protein Digestion and Purification with Membranes Attached to Pipet Tips. *Anal. Chem.* **2015**, *87* (24), 11984–11989. https://doi.org/10.1021/acs.analchem.5b03679.

(29) *Trypsin Spin Columns for Proteomics Immobilized Trypsin*. http://www.sigmaaldrich.com/ (accessed 2022-11-24).

(30) *Immobilized Trypsin*. https://www.promega.com/products/mass-spectrometry/trypsin/immobilized-trypsin/ (accessed 2022-11-24).

(31) Dong, J.; Migliore, N.; Mehrman, S. J.; Cunningham, J.; Lewis, M. J.; Hu, P. High-Throughput, Automated Protein A Purification Platform with Multiattribute LC–MS Analysis for Advanced Cell Culture Process Monitoring. *Anal. Chem.* **2016**, *88* (17), 8673–8679. https://doi.org/10.1021/acs.analchem.6b01956.

(32) *Empty Spin Columns*. Bio-Rad Laboratories. https://www.bio-rad.com/en-us/product/empty-spin-columns?ID=612dbf40-5acd-468f-8eef-b855ce941865 (accessed 2022-11-25).

(33) Lippold, S.; Büttner, A.; Choo, M. S. F.; Hook, M.; de, C. J.; Nguyen-Khuong, T.; Haberger, M.; Reusch, D.; Wuhrer, M.; de Haan, N. Cysteine Aminoethylation Enables Site-Specific Glycosylation Analysis of Recombinant Human Erythropoietin Using Trypsin. Anal. Chem. 2020, 92 (14), 9476–9481. https://doi.org/10.1021/acs.analchem.0c01794.

(34) Fang, Z.; Qin, H.; Mao, J.; Wang, Z.; Zhang, N.; Wang, Y.; Liu, L.; Nie, Y.; Dong, M.; Ye, M. Glyco-Decipher Enables Glycan Database-Independent Peptide Matching and in-Depth Characterization of Site-Specific N-Glycosylation. *Nat. Commun.* **2022**, *13* (1), 1900. https://doi.org/10.1038/s41467-022-29530-y.

(35) Zeng, W.-F.; Cao, W.-Q.; Liu, M.-Q.; He, S.-M.; Yang, P.-Y. Precise, Fast and Comprehensive Analysis of Intact Glycopeptides and Modified Glycans with PGlyco3. *Nat. Methods* **2021**, *18* (12), 1515–1523. https://doi.org/10.1038/s41592-021-01306-0.

(36) Go, E. P.; Zhang, S.; Ding, H.; Kappes, J. C.; Sodroski, J.; Desaire, H. The Opportunity Cost of Automated Glycopeptide Analysis: Case Study Profiling the SARS-CoV-2 S Glycoprotein. *Anal. Bioanal. Chem.* **2021**, *413* (29), 7215–7227. https://doi.org/10.1007/s00216-021-03621-z.

(37) Wang, B.; Tsybovsky, Y.; Palczewski, K.; Chance, M. R. Reliable Determination of Site-Specific In Vivo Protein ***N*** - Glycosylation Based on Collision-Induced MS/MS and Chromatographic Retention Time. *J. Am. Soc. Mass Spectrom.* **2014**, *25* (5), 729–741. https://doi.org/10.1007/s13361-013-0823-6.

(38) Klein, J.; Zaia, J. Relative Retention Time Estimation Improves N-Glycopeptide Identifications by LC–MS/MS. *J. Proteome Res.* **2020**, *19* (5), 2113–2121. https://doi.org/10.1021/acs.jproteome.0c00051.

(39) Choo, M. S.; Wan, C.; Rudd, P. M.; Nguyen-Khuong, T. GlycopeptideGraphMS: Improved Glycopeptide Detection and Identification by Exploiting Graph Theoretical Patterns in Mass and Retention Time. *Anal. Chem.* **2019**, *91* (11), 7236–7244. https://doi.org/10.1021/acs.analchem.9b00594.

(40) Rogstad, S.; Yan, H.; Wang, X.; Powers, D.; Brorson, K.; Damdinsuren, B.; Lee, S. Multi-Attribute Method for Quality Control of Therapeutic Proteins. *Anal. Chem.* **2019**, *91* (22), 14170–14177. https://doi.org/10.1021/acs.analchem.9b03808.

(41) Pais, D. A. M.; Carrondo, M. J.; Alves, P. M.; Teixeira, A. P. Towards Real-Time Monitoring of Therapeutic Protein Quality in Mammalian Cell Processes. *Curr. Opin. Biotechnol.* **2014**, *30*, 161–167. https://doi.org/10.1016/j.copbio.2014.06.019.

(42) van der Burgt, Y. E. M.; Siliakus, K. M.; Cobbaert, C. M.; Ruhaak, L. R. HILIC–MRM–MS for Linkage-Specific Separation of Sialylated Glycopeptides to Quantify Prostate-Specific Antigen Proteoforms. *J. Proteome Res.* **2020**, *19* (7), 2708–2716. https://doi.org/10.1021/acs.jproteome.0c00050.

(43) Zhong, J.; Huang, Y.; Mechref, Y. Derivatization of Sialylated Glycopeptides (DOSG) Enabling Site-Specific Isomeric Profiling Using LC-MS/MS. *Anal. Chem.* **2021**, *93* (14), 5763–5772. https://doi.org/10.1021/acs.analchem.0c05149.

(44) Nwosu, C. C.; Strum, J. S.; An, H. J.; Lebrilla, C. B. Enhanced Detection and Identification of Glycopeptides in Negative Ion Mode Mass Spectrometry. *Anal. Chem.* **2010**, *82* (23), 9654–9662. https://doi.org/10.1021/ac101856r.

(45) DeGraan-Weber, N.; Reilly, J. P. Use of Cysteine Aminoethylation To Identify the Hypervariable Peptides of an Antibody. *Anal. Chem.* **2018**, *90* (3), 1608–1612. https://doi.org/10.1021/acs.analchem.7b02732.

(46) Shrivastava, A.; Joshi, S.; Guttman, A.; Rathore, A. S. N-Glycosylation of Monoclonal Antibody Therapeutics: A Comprehensive Review on Significance and Characterization. *Anal. Chim. Acta* **2022**, *1209*, 339828. https://doi.org/10.1016/j.aca.2022.339828.

(47) Gargano, A. F. G.; Schouten, O.; van Schaick, G.; Roca, L. S.; van den Berg-Verleg, J. H.; Haselberg, R.; Akeroyd, M.; Abello, N.; Somsen, G. W. Profiling of a High Mannose-Type N-Glycosylated Lipase Using Hydrophilic Interaction Chromatography-Mass Spectrometry. *Anal. Chim. Acta* **2020**, *1109*, 69–77. https://doi.org/10.1016/j.aca.2020.02.042.

(48) Schnier, P. D.; Gross, D. S.; Williams, E. R. On the Maximum Charge State and Proton Transfer Reactivity of Peptide and Protein Ions Formed by Electrospray Ionization. *J. Am. Soc. Mass Spectrom.* **1995**, *6* (11), 1086–1097. https://doi.org/10.1016/1044-0305(95)00532-3.

(49) Liigand, P.; Kaupmees, K.; Kruve, A. Influence of the Amino Acid Composition on the Ionization Efficiencies of Small Peptides.

J. Mass Spectrom. **2019**, *54* (6), 481–487. https://doi.org/10.1002/jms.4348.

(50) Malthouse, J. P. G. Kinetic Studies of the Effect of pH on the Trypsin-Catalyzed Hydrolysis of *N* -α-Benzyloxycarbonyl- L -Lysine- *p* -Nitroanilide: Mechanism of Trypsin Catalysis. *ACS Omega* **2020**, *5* (10), 4915–4923. https://doi.org/10.1021/acsomega.9b03750.

(51) Reusch, D.; Haberger, M.; Falck, D.; Peter, B.; Maier, B.; Gassner, J.; Hook, M.; Wagner, K.; Bonnington, L.; Bulau, P.; Wuhrer, M. Comparison of Methods for the Analysis of Therapeutic Immunoglobulin G Fc-Glycosylation Profiles—Part 2: Mass Spectrometric Methods. *mAbs* **2015**, *7* (4), 732–742. https://doi.org/10.1080/19420862.2015.1045173.

(52) Sanchez-De Melo, I.; Grassi, P.; Ochoa, F.; Bolivar, J.; García-Cózar, F. J.; Durán-Ruiz, M. C. N-Glycosylation Profile Analysis of Trastuzumab Biosimilar Candidates by Normal Phase Liquid Chromatography and MALDI-TOF MS Approaches. *J. Proteomics* **2015**, *127*, 225–233. https://doi.org/10.1016/j.jprot.2015.04.012.

(53) Kolarich, D.; Jensen, P. H.; Altmann, F.; Packer, N. H. Determination of Site-Specific Glycan Heterogeneity on Glycoproteins. *Nat. Protoc.* **2012**, *7* (7), 1285–1298. https://doi.org/10.1038/nprot.2012.062.

(54) Keil, B. Specificity of Proteolysis; Springer-Verlag: Berlin, Germany, 1992.

(55) Zhao, P.; Praissman, J. L.; Grant, O. C.; Cai, Y.; Xiao, T.; Rosenbalm, K. E.; Aoki, K.; Kellman, B. P.; Bridger, R.; Barouch, D. H.; Brindley, M. A.; Lewis, N. E.; Tiemeyer, M.; Chen, B.; Woods, R. J.; Wells, L. Virus-Receptor Interactions of Glycosylated SARS-CoV-2 Spike and Human ACE2 Receptor. *Cell Host Microbe* **2020**, *28* (4), 586-601.e6. https://doi.org/10.1016/j.chom.2020.08.004.

(56) Zhang, Y.; Zhao, W.; Mao, Y.; Chen, Y.; Wang, S.; Zhong, Y.; Su, T.; Gong, M.; Du, D.; Lu, X.; Cheng, J.; Yang, H. Site-Specific N-Glycosylation Characterization of Recombinant SARS-CoV-2 Spike Proteins. *Mol. Cell. Proteomics* **2021**, *20*, 100058. https://doi.org/10.1074/mcp.RA120.002295.

(57) Sanda, M.; Morrison, L.; Goldman, R. N- and O-Glycosylation of the SARS-CoV-2 Spike Protein. *Anal. Chem.* **2021**, *93* (4), 2003–2009. https://doi.org/10.1021/acs.analchem.0c03173.

(58) Pompach, P.; Brnakova, Z.; Sanda, M.; Wu, J.; Edwards, N.; Goldman, R. Site-Specific Glycoforms of Haptoglobin in Liver Cirrhosis and Hepatocellular Carcinoma. *Mol. Cell. Proteomics* **2013**, *12* (5), 1281–1293. https://doi.org/10.1074/mcp.M112.023259.

(59) Huang, J.; Wang, D.; Shipman, R. D.; Zhu, Z.; Liu, Y.; Li, L. Simultaneous Enrichment and Separation of Neutral and Sialyl Glycopeptides of SARS-CoV-2 Spike Protein Enabled by Dual-Functionalized Ti-IMAC Material. *Anal. Bioanal. Chem.* **2021**, *413* (29), 7295–7303. https://doi.org/10.1007/s00216-021-03433-1.

(60) Coutinho, M. F.; Prata, M. J.; Alves, S. Mannose-6-Phosphate Pathway: A Review on Its Role in Lysosomal Function and Dysfunction. *Mol. Genet. Metab.* **2012**, *105* (4), 542–550. https://doi.org/10.1016/j.ymgme.2011.12.012.

(61) Huang, J.; Dong, J.; Shi, X.; Chen, Z.; Cui, Y.; Liu, X.; Ye, M.; Li, L. Dual-Functional Titanium(IV) Immobilized Metal Affinity Chromatography Approach for Enabling Large-Scale Profiling of Protein Mannose-6-Phosphate Glycosylation and Revealing Its Predominant Substrates. *Anal. Chem.* **2019**, *91* (18), 11589–11597. https://doi.org/10.1021/acs.analchem.9b01698.

For Table of Contents Use Only

Analysis of protein glycosylation after rapid digestion using protease-containing membranes in spin columns

Weikai Cao and Merlin L. Bruening

The graphic depicts 30-second digestion of a protein during passage through a protease-containing spin-membrane. Subsequent LC-MS/MS analysis enables site-specific identification of glycans.